JOURNAL OF VIROLOGY, Mar. 2002, p. 2340–2349 Vol. 76, No. 5
0022-538X/02/$04.00+0 DOI: 10.1128/JVI.76.5.2340–2349.2002

Endocytosis of Adeno-Associated Virus Type 5 Leads to Accumulation of Virus Particles in the Golgi Compartment

Ursula Bantel-Schaal,[1]* Birgit Hub,[1] and Juergen Kartenbeck[2]

Forschungsschwerpunkt Angewandte Tumorvirologie F0400, Abteilung Pathogenitätsmechanismen,[1] and Forschungsschwerpunkt Krebsentstehung und Differenzierung A0100, Abteilung für Zellbiologie,[2] Deutsches Krebsforschungszentrum Heidelberg, 69120 Heidelberg, Germany

Received 7 November 2001/Accepted 19 November 2001

Among the adeno-associated virus (AAV) serotypes which are discussed as vectors for gene therapy AAV type 5 (AAV5) represents a candidate with unique advantages. To further our knowledge on AAV5-specific characteristics, we studied the entry pathway of wild-type virus in HeLa cells in the absence of helper virus by immunofluorescence and electron microscopy and by Western blot analysis. We found virus binding at the apical cell surface, especially at microvilli and, with increasing incubation time, virus accumulation at cell-cell boundaries. The different binding kinetics suggest different binding properties at apical versus lateral plasma membranes. Endocytosis of viruses was predominantly by clathrin-coated vesicles from both membrane domains; however, particles were also detected in noncoated pits. AAV5 particles were mainly routed to the Golgi area, where they could be detected within cisternae of the trans-Golgi network and within vesicles associated with cisternae and with the dictyosomal stacks of the Golgi apparatus. These data suggest that AAV5 makes use of endocytic routes that have hitherto not been described as pathways for virus entry.

Adeno-associated viruses (AAVs) are small, nonenveloped parvoviruses which depend on a viral helper for productive infection (for a review see reference 8). Up to now, six primate serotypes (AAV type 1 [AAV1] to AAV6) have been reported (2, 11, 50, 53).

Most of the experimental data derived from work with AAV2 (for reviews see references 8 and 36). In the absence of a helper virus wild-type AAV2 integrates in a site-specific manner into human chromosome 19 and establishes a latent infection (34, 51). Site specificity requires expression of one of the large nonstructural AAV2 Rep proteins (1, 58). In the absence of Rep proteins concatemers or interlocked circles may form and can persist in an episomal form, thus mediating long-term expression in vivo (18, 60). Because of these properties and the broad host ranges of the viruses and because no AAV-based pathology has been shown (for reviews see references 8 and 36), these viruses are being tested as gene therapy vectors (for reviews see references 24, 42, and 54). However, the use of AAV2 vectors also involves disadvantages as not all target cells are permissive for AAV2 (46, 66) and a significant level of immunity exists in human populations (20, 21, 40). Furthermore, neutralizing antibodies block readministration of AAV2-derived vectors in animals (7, 13, 26, 39). Thus efforts have been made to test other AAV serotypes to overcome these difficulties 9, 12, 43, 50, 65, 67; for a review, see reference 23).

Among these serotypes AAV5 is a candidate with a number of advantages: (i) AAV5 has been shown to infect target cells that are of interest for gene transfer but that are not permissive for AAV2 (14, 67), (ii) it is only distantly related to all other known serotypes (2, 11), and (iii) it represents the only serotype originally isolated from human material and not from helper adenovirus stocks (3, 21). Since virtually nothing is known about the uptake and intracellular trafficking of AAV5, we investigated the entry pathway of this virus using the well-established human HeLa cell line, which is known to allow propagation of AAV5.

* Corresponding author. Mailing address: Forschungsschwerpunkt Angewandte Tumorvirologie F0400, Abteilung Pathogenitätsmechanismen, Deutsches Krebsforschungszentrum Heidelberg, Im Neuenheimer Feld 242, 69120 Heidelberg, Germany. Phone: 49-6221-424823. Fax: 49-6221-424902. E-mail: u.bantel-schaal@dkfz-heidelberg.de.

MATERIALS AND METHODS

Cells and culture. HeLa cells were grown as monolayers in Dulbecco's minimal essential medium (Sigma) supplemented with 10% fetal calf serum, penicillin-streptomycin, and glutamine (Gibco-BRL, Paisley, Scotland) at standard concentrations.

Virus and virus infection. AAV5 was propagated in HeLa cells with the helper adenovirus type 2 and was purified using ammonium sulfate precipitation and ultracentrifugation as described previously (3). The infectious titer was determined by dot blotting HeLa cells that had been coinfected with AAV5 serially diluted by a factor of 10 and constant amounts of adenovirus type 2 (helper virus) on GeneScreen filters (NEN, Cologne, Germany). The filters were hybridized with radiolabeled AAV5 DNA (4). Physical particle titers were determined by estimating AAV5 DNA amounts from agarose gels. They were on the order of 10^3 times the infectious titer.

Infection with a dose of 10^2 to 10^3 infectious AAV5 particles/cell (corresponding to 10^5 to 10^6 physical particles) was at 37°C for various periods of time (20 min, 45 min, 90 min, 3 h, 6 h, and 22 h). For infection periods longer than 90 min the inoculum was removed and, after three washes, was replaced by fresh medium.

Antibodies. Mouse monoclonal antibodies against AAV5 capsids (clone B4) and rabbit polyclonal antisera against Golgi α-mannosidase II (ManII) are described elsewhere (21, 59). Mouse monoclonal antibody B1 (64) (a kind gift from J. Kleinschmidt, Deutsches Krebsforschungszentrum Heidelberg), which recognizes the capsid proteins of all AAV serotypes in Western blots, was used for immunoblot reactions. Mouse monoclonal antibodies against human EEA1 were from Transduction Laboratories, and the secondary antibodies Alexa 488 anti-mouse and Cy3 antirabbit were from Dianova (Hamburg, Germany). Horseradish peroxidase-coupled goat anti-mouse antibodies used for enhanced chemiluminescence detection in Western blots and goat anti-mouse antibodies coupled to 5-nm gold-particles used in immunoelectron microscopy were from Amersham Life Science.

Immunofluorescence. For immunofluorescence HeLa cells were grown on coverslips. At various times postinfection (p.i.) the cells were fixed either at −20°C in 100% methanol (10 min) followed by 100% acetone (a few seconds) or in 2.5% formaldehyde in phosphate-buffered saline (PBS; freshly prepared from paraformaldehyde), pH 7.2, at room temperature for 15 min. Formaldehyde treatment was followed by three washes with 50 mM ammonium chloride (in PBS) to block free aldehyde groups, and cells were treated for permeabilization with 0.1% saponin in PBS (5 min). Fluorescence imaging micrographs were taken with an Axiophot microscope (Carl Zeiss, Jena, Germany). Confocal laser scanning microscopy was performed using an LSM510 apparatus (Carl Zeiss, Oberkochen, Germany). For double fluorescence an argon ion laser (488 nm) and an HeNe laser (543 nm) with corresponding barrier filters in the double-track mode of the instrument (i.e., each scan line was alternatively illuminated with only one wavelength) were used.

All antibodies were diluted in PBS (anti-AAV5 capsids, 1:200; anti-EEA1, 1:50, anti-ManII, 1:400; Cy3 antirabbit, 1:150; Alexa 488 antimouse, 1:250). Incubation with antibodies (30 min each) and washings (three times between each step with PBS) were done at room temperature. Air-dried coverslips were mounted with Elvanol.

Transmission electron microscopy. HeLa cells grown on coverslips were infected with AAV5 for various periods of time (as indicated above) and were fixed at room temperature in 2.5% glutaraldehyde (in 50 mM cacodylate buffer [pH 7.2], 50 mM KCl, 2.5 mM $MgCl_2$) for 30 min, followed by 1 h in 2% OsO_4 (in 50 mM cacodylate buffer) and by overnight treatment with 0.5% aqueous uranyl acetate prior to dehydration and embedding (32).

Electron-microscopic immunolocalization. For preembedding immunolocalization, infected HeLa cells were fixed with formaldehyde as described above for immunofluorescence except that the formaldehyde concentration was raised to 3% and fixation was for 20 min. For permeabilization, 0.05% saponin was used for 3 min. The monoclonal anti-AAV5 capsid antibody was applied for 2 to 4 h followed by an overnight incubation with the diluted (1:5 in PBS) gold-labeled secondary antibody. After three washes with PBS the cells were fixed as described for routine electron microscopy (32, 33).

Negative staining. For negative staining of diluted AAV5 preparations we used freshly glow-discharged, carbon-coated grids and 2% uranyl acetate in aqueous solution.

Western blotting. Infected cells were washed twice with cold PBS containing a cocktail of serine- and cysteine-inhibiting proteases (Roche, Mannheim, Germany) suited for the protection of proteins isolated from animal tissues. The cells were scraped off the dish using sodium dodecyl sulfate (SDS) sample buffer (35) containing 0.1% Benzonase (Merck), carefully homogenized, heated, and separated by SDS-polyacrylamide gel electrophoresis (35). The separated proteins were electroblotted onto polyvinylidene difluoride membranes. Blocking (30 min) and incubation with the primary and secondary antibodies (60 min each) were carried out in 5% fat-free milk in PBS. Washings were done in 0.3% Tween 20 in PBS. Detection of the immunoreaction was performed using the ECL system (Amersham).

RESULTS

To study the entry pathway of AAV5, we infected HeLa cells with 10^2 to 10^3 infectious particles (corresponding to 10^5 to 10^6 physical particles) per cell. As revealed by negative staining the AAV5 preparation used for the studies consisted of a homogenous population of intact virus particles uniformly about 23 nm in diameter (Fig. 1a). Empty capsids were only rarely detected. To ascertain AAV5 identity of the small particles on the cellular background, we performed immunoelectron microscopy (Fig. 1b to f) using gold-labeled secondary antibodies. AAV5 particles (Fig. 1) could be identified as single particles or densely clustered particles on microvilli (Fig. 1b to d), in coated pits (Fig. 1e) and coated vesicles (Fig. 1f), and on the cell surface (Fig. 1f). Within the cell, detection of gold-labeled virus particles proved difficult when the targets were cellular structures surrounded by a distinct membrane. Since the integrity of membranes is affected by the saponin treatment required to allow access of the antibodies, detection of gold label is associated with more or less damaged organelles. Examples of disintegrated structures representing early endosomes and lysosomes with some gold label indicating AAV5 particles are shown in Fig. 1g to i. Figure 1g to i also indicate that, although morphology is affected, the gold localization is specific for AAV5 particles (Fig. 1b to i), and thus cellular structures of comparable size (e.g., free or membrane-bound ribosomes) and others were not labeled (Fig. 1h and i).

When HeLa cells were incubated with AAV5 for various periods of time and were then analyzed by immunofluorescence microscopy, staining could be seen at different cellular locations (Fig. 2). Within 20 and 90 min p.i. staining intensity increased at the cell periphery, suggesting predominant virus binding at cell-to-cell boundaries (Fig. 2a to c). In addition a more dotted distribution of fluorescence signals over the entire cell surface was seen (Fig. 2b and c). After 6 h, the signals at the cell peripheries were markedly reduced but staining was still spread over the entire cell (Fig. 2d). In some cells, concentration of fluorescence signals in cap-like structures in a juxtanuclear position was also seen (Fig. 2d). At 22 h p.i. these perinuclear caps exhibited the predominant signals in almost all cells (Fig. 2e). In addition, very faint fluorescence signals could be seen occasionally at the nuclear membrane (Fig. 2e), but no AAV5-specific immunostaining was detected within the cell nucleus.

To further characterize the cellular compartment which accounts for the perinuclear caps, we performed double-label confocal laser scanning microscopy at 2 and 22 h p.i. using antibodies specific for the medial cisternae of the Golgi apparatus (Golgi ManII) and against AAV5 capsids (Fig. 3). At 2 h p.i. the distributions of fluorescence signals for AAV5 capsids and ManII clearly differed (Fig. 3a to c), but at 22 h p.i. (Fig. 3d to f) the merged signals showed some colocalization in cap-like structures located close to the cell nucleus, suggesting that AAV5 particles accumulated in the Golgi area. The fluorescence signals showing up with endosome-specific antibodies did not aggregate to perinuclear caps and differed clearly in location from those obtained for ManII and for AAV5 capsids (Fig. 3g to i).

Electron micrographs taken at times identical to those described in the immunofluorescence studies allowed elucidation of the various steps of the endocytic pathway of AAV5 in more detail. Early after addition (20 min) virus particles were occasionally seen between neighboring cells (not shown), bound to the surface of the cell body and to microvilli, and in coated pits (Fig. 4a to c). The binding forces of the virus often seemed to fix microvilli to each other or to the cell surface (Fig. 4a and b). Beginning at about 45 min p.i. coated vesicles containing numerous virus particles were found frequently (Fig. 4d to g). AAV5 particles were also detectable in tubular structures that are likely to represent early endosomes (Fig. 4f). In rare situations endocytosis via noncoated vesicles, probably representing caveolae, was also seen (Fig. 4h and i). Increasing amounts of tightly packed virus particles bound to lateral surfaces (identified by desmosomal structures; Fig. 4k) and endocytosis by coated vesicles from these intercellular spaces appeared at later time points (Fig. 4k to o; 90 min).

Between 3 and 6 h after application, the internalized virus was detected in the Golgi area (Fig. 5). Virus was seen close to the Golgi network in clathrin-coated vesicles (Fig. 5a, d, and h) and in membrane tubules of uniform diameter (Fig. 5b and e).

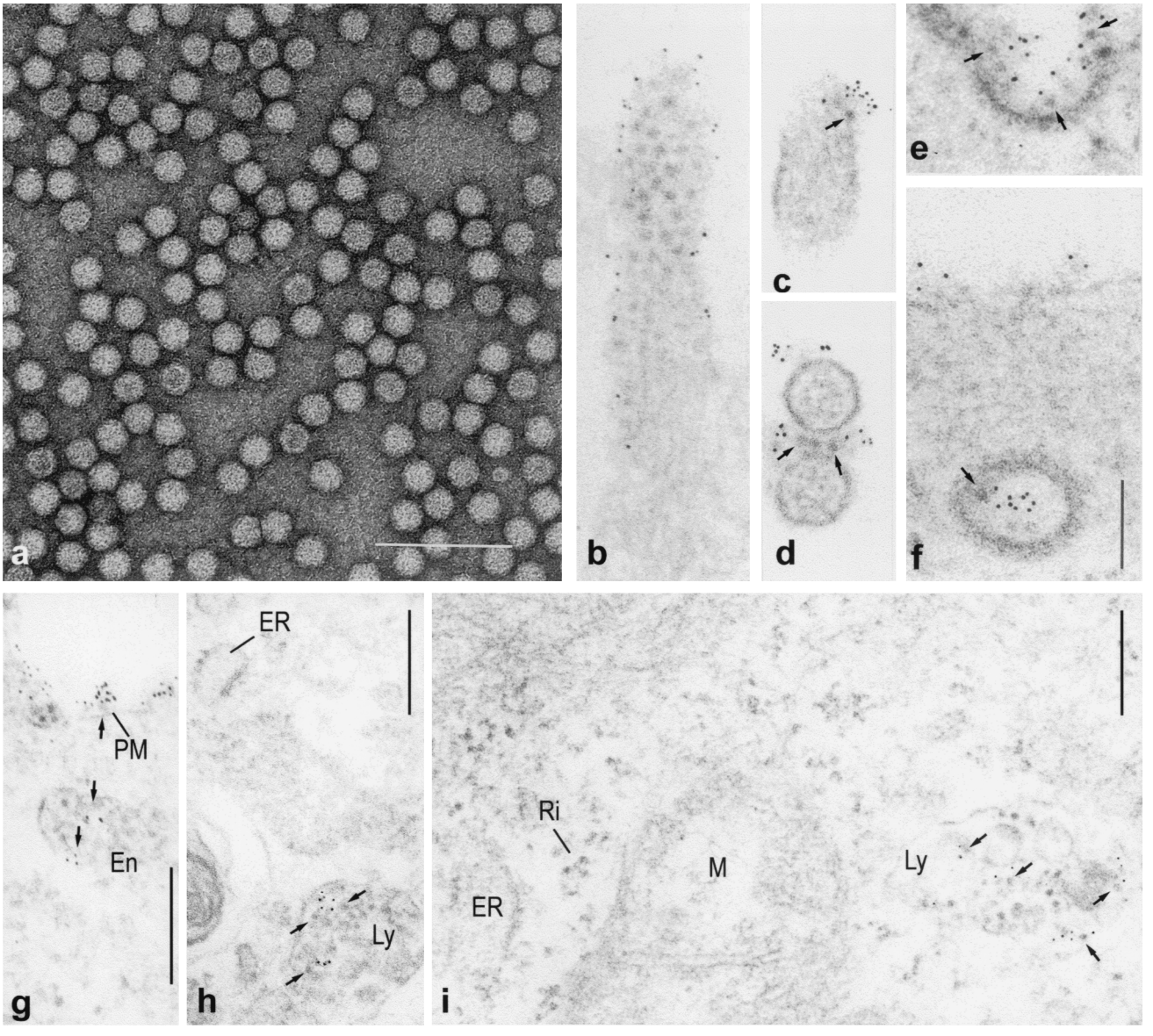

FIG. 1. (a) AAV5 particles negatively stained with 2% uranyl acetate in aqueous solution. Bar, 0.1 μm. (b to f) Electron-microscopic immunolocalization of AAV5 in HeLa cells. Cells were infected with AAV5 at 37°C and fixed with formaldehyde 90 min p.i. Immunoreactions were done using a monoclonal antibody specific for AAV5 capsids (21) and anti-mouse antibodies coupled to 5-nm gold particles for visualization. Since they were done prior to cell embedding, labeling could be detected only when AAV particles were accessible to the antibodies in the preembedding state. Thus only the laterally located particles in the flat section (b and c) are labeled with gold. Arrows, virus particles on (b and c) and between (d) microvilli, in a coated pit (e), in a coated vesicle (f), within an endosome (g), and within lysosomal structures (h and i). The concentration of AAV5 used in the experiments shown in panels e to i was 10-fold higher than that used in experiments shown in panels b to d. En, endosome; ER, rough endoplasmic reticulum; Ly, lysosomal structure; M, mitochondrion; PM, plasma membrane; Ri, ribosomes; Bars, 0.1 μm (f; applies to panels b to f) and 0.2 μm (i; applies to panels g to i).

Furthermore, virus particles were detected in cisternae of the trans-Golgi network (TGN) (Fig. 5c, d, f, h, and i), identifiable by the characteristic clathrin- and coatomer-coated vesicles (Fig. 5h and i). After prolonged incubation (22 h) AAV5 could additionally be seen in noncoated larger vesicles located close to dilated cisternae and the stacks of the Golgi apparatus (Fig. 5g). In contrast, AAV5 was not found in lysosomes under the conditions used and described above. Only when the number of infectious particles was further increased (e.g., to 10^4 infectious particles/cell) did AAV5 accumulate in lysosomes (Fig. 1h and i) in addition to the Golgi areas. Neither release of intact virus particles into the cytoplasm from any of the described virus-containing compartments nor intact virus particles in the cytoplasm could be verified. Also, no intact virus particles at nuclear pores or within the cell nucleus were detected by electron microscopy.

To allow an estimation of bound and endocytosed virus versus degraded virus, we performed Western blot analysis using total cell lysates of infected HeLa cells. In agreement with the immunofluorescence and electron microscopic data,

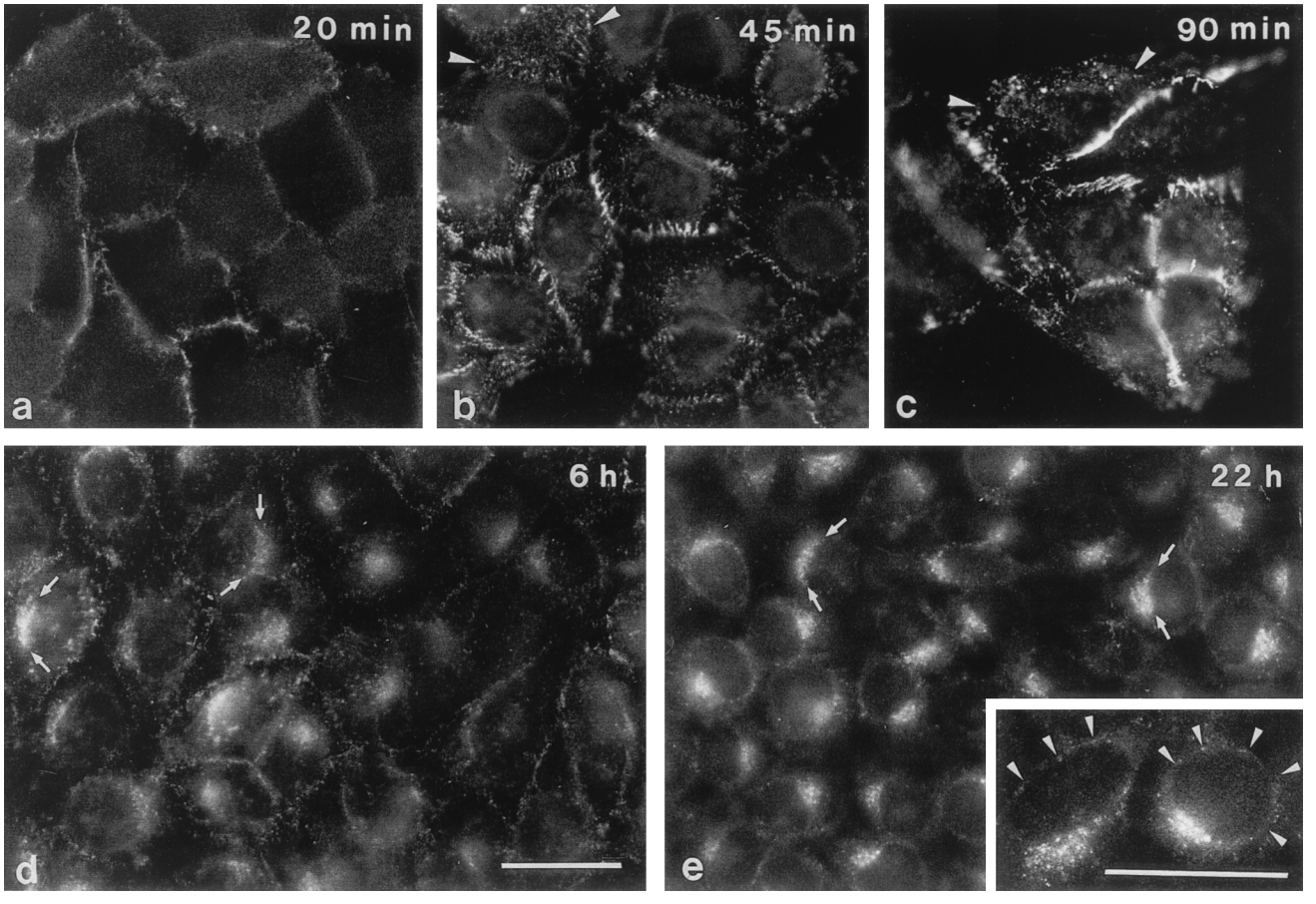

FIG. 2. Immunofluorescence microscopy of HeLa cells after incubation with AAV5. HeLa cells were cultured in the presence of AAV5 for the indicated periods of time and were then fixed with methanol-acetone before incubation with antibodies. Removal of the inoculum was after 90 min (c) and was followed by three washes before addition of fresh medium. Arrowheads (b and c), viruses at apical cell surfaces and in endocytic structures; arrows (d and e), fluorescent aggregates in juxtanuclear position. Inset (e), additional faint positive reactions at the nuclear envelope (arrowheads). Bars (d and inset), 30 μm (the bar in panel d applies to panels a to e [except for the inset]).

immunoblotting revealed that the amount of cell-associated AAV5 increased with time (Fig. 6; 20, 45, and 90 min). After the inoculum was replaced by fresh medium, bound and/or internalized viral protein could still be identified in the course of the whole experiment (up to 22 h p.i.), albeit with decreasing intensity (Fig. 6).

DISCUSSION

After animal viruses bind to a receptor(s) at the surface of a host cell, their entry into the interior of the cell is initiated by direct fusion of the virus with the cell surface or by receptor-mediated endocytosis via clathrin-coated pits and vesicles and via small noncoated vesicles (e.g., caveolae). These initial steps are required for entry of enveloped and of nonenveloped viruses (10, 29, 32, 55; for a recent review see reference 28).

Our study (schematically summarized in Fig. 7) suggests two types of binding sites for AAV5 on HeLa cells. One, at the apical cell surface, appears to be restricted in number and becomes transiently exhausted during internalization and recycling. The other, at lateral sites, may provide a high binding capacity, thus allowing binding and uptake of large amounts of AAV5 over an extended period of time. The nature of the binding sites used by AAV5 are still unknown. For AAV2 heparan sulfate proteoglycan (HSPG) is reported to be the primary virus attachment receptor (57), and $\alpha_V\beta_5$ integrin and human fibroblast growth factor receptor 1 are said to function as coreceptors (47, 56) although there exists still some controversy about the importance of both HSPG and $\alpha_V\beta_5$ integrin (48, 49). In contrast to AAV2 infection, AAV5 infection does not depend on heparan sulfate but appears to require 2,3-linked sialic acid (63). There are no data as to the possible dependence of AAV5 on $\alpha_V\beta_5$ integrin and human fibroblast growth factor receptor 1.

Our data show that entry of AAV5 in HeLa cells occurs predominantly via coated pits and coated vesicles although virus particles in noncoated pits and vesicles were also observed occasionally. Thus more than one entry mechanism can be used by one type of virus for entering the same type of cells. This may explain the differences observed in parvovirus uptake. For viruses of this group, e.g., the helper virus-dependent AAV2 and AAV2-derived recombinants and the autonomous canine parvovirus (CPV), clathrin-mediated endocytosis has been reported (5, 45) but uptake of CPV via uncoated vesicles has also been shown (6). Involvement of dynamin in AAV2

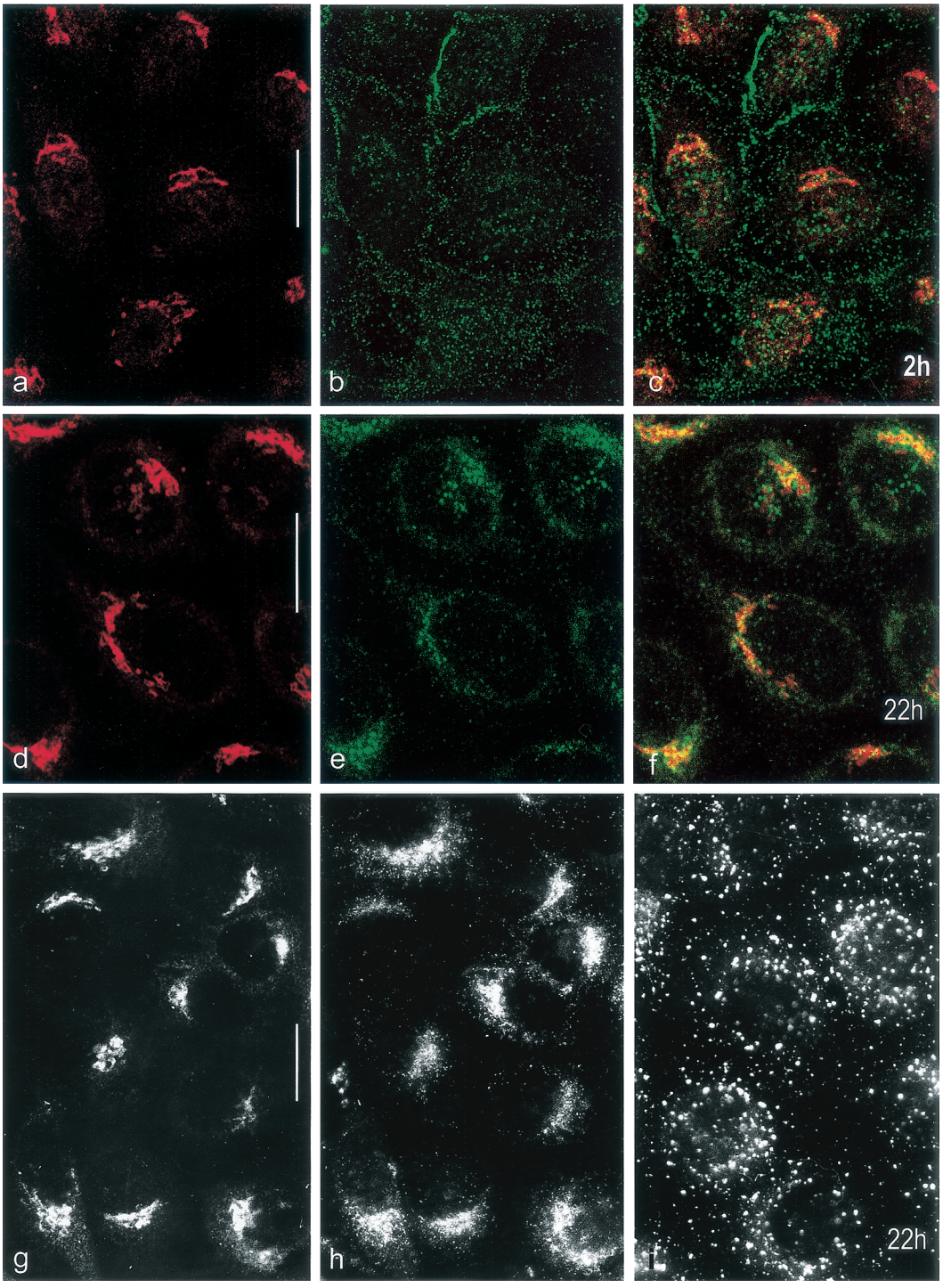

FIG. 3. Distribution of fluorescence signals on AAV5-infected HeLa cells. HeLa cells were infected with AAV5 for 2 (a to c) and 22 h (d to i). At the times indicated cells were fixed with methanol-acetone (a to f) or with formaldehyde (g to i). Double labeling (confocal laser scanning microscopy; optical sections, 0.6 μm thick) (a to f) was done using primary antibodies specific for Golgi ManII (a and d) and for AAV5 capsids (b and e). The respective merged images are shown in panels c and f. The images in panels g to i show that the signal distributions for antibodies to ManII (g) and AAV5 capsids (h) are different from that for the antibody to EEA1 (endosomes) (i) at 22 h p.i. Formaldehyde fixation was used (g to i) to verify the results obtained with methanol-acetone fixation. Bars, 20 μm.

and CPV infection (17, 45) did not help to clarify the situation since dynamin appears to mediate more than one endocytotic process (30, 41).

While numerous coated vesicles containing viruses were seen throughout incubation periods of several hours, AAV5 particles in typical lysosomal structures were only detected when the particle concentration was raised beyond our standard level, which might be an indication of saturation of main

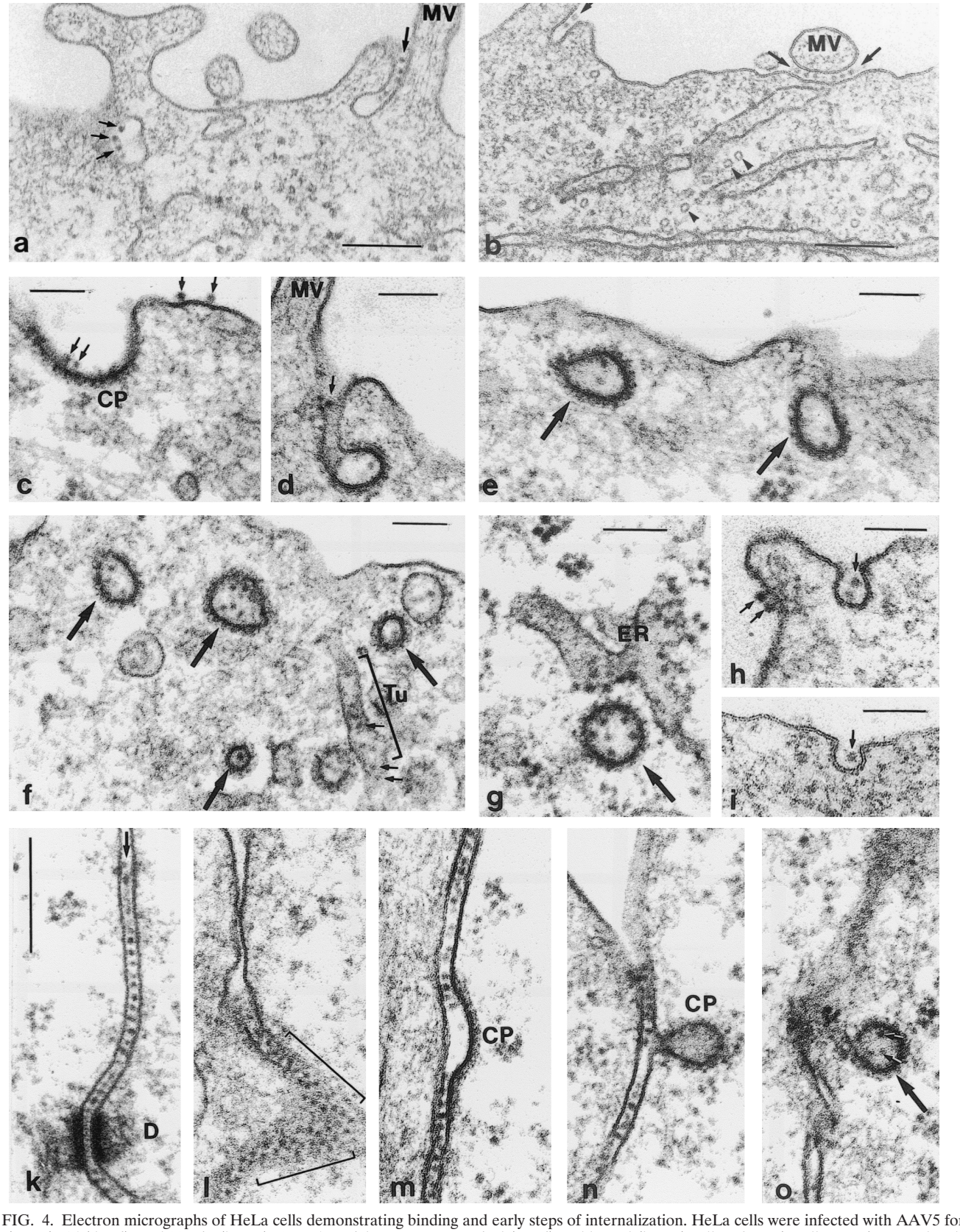

FIG. 4. Electron micrographs of HeLa cells demonstrating binding and early steps of internalization. HeLa cells were infected with AAV5 for 20 (a to c), 45 (d to i), and 90 min (k to o). AAV5 particles are seen at apical (a to i) and lateral (k to o) cell surfaces (small arrows). Arrowheads (b), cross-sectioned microtubules as an internal size marker. Internalization of viruses by coated vesicles takes place from apical (c to g) and lateral (m to o) cell surfaces (large arrows). Tu (f), example of particles in tubular structures that are likely to represent early endosomes. Aggregated viruses at lateral surfaces are demonstrated in cross (k, m, and n) and oblique (l, brackets) sections. In rare situations internalization via noncoated pits and vesicles was also seen (h and i). CP, coated pit; ER, endoplasmic reticulum; MV, microvilli; D, desmosome. Bars, 0.2 μm (a, b, and k; same magnification for panels k to o) and 0.1 μm (c to i).

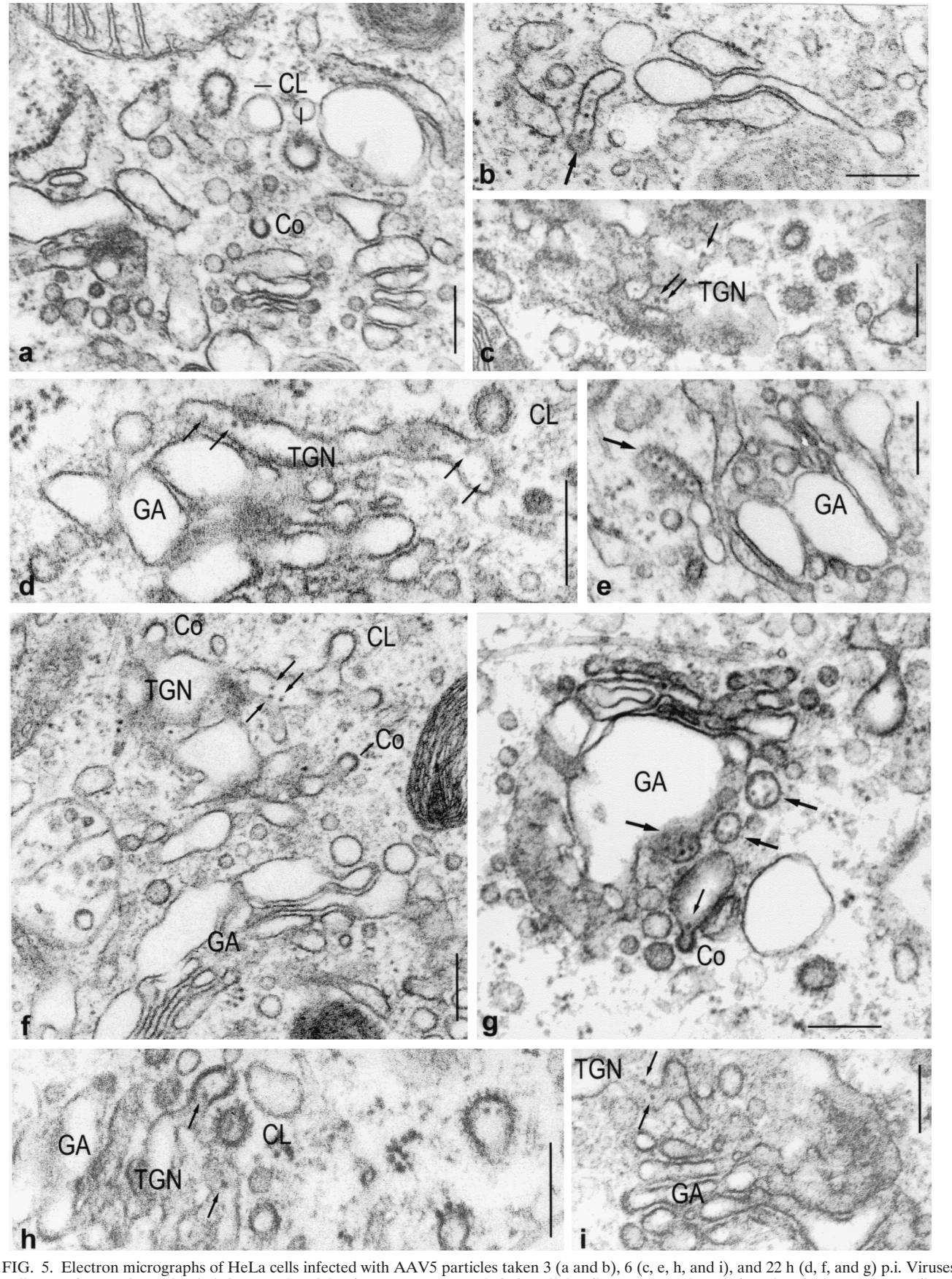

FIG. 5. Electron micrographs of HeLa cells infected with AAV5 particles taken 3 (a and b), 6 (c, e, h, and i), and 22 h (d, f, and g) p.i. Viruses (small arrows) were found in clathrin-coated vesicles (CL; see, e.g., panel a), in tubular (large arrows; b and e) and vesicular structures (large arrows; g), and in noncoated vesicles in the vicinity of dilated Golgi cisternae and stacks of the Golgi apparatus (GA; large arrows). Examples of cisternae of the TGN containing AAV5 particles are given in panels c, d, g, h, and i. Co, coatomer-coated vesicles. Bars, 0.2 μm.

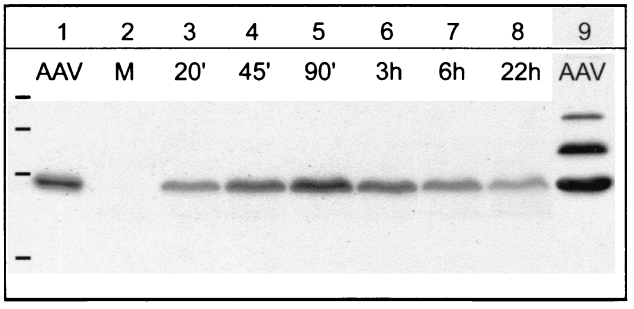

FIG. 6. Western blot analysis of HeLa cell proteins after incubation with AAV5 particles. After the indicated periods of time (lanes 3 to 8) cells were washed and homogenized. Equal amounts of proteins (cells) were loaded onto the gel. After 90 min the inoculum was replaced by fresh virus-free culture medium (lanes 6 to 8). Lane 1, calculated virus concentration used in infection. A 10-fold concentration (lane 9) was used to demonstrate that the antibody recognizes all three capsid proteins. Lane 2, mock-infected cells.

targets. Instead viruses were detected in the Golgi area, especially in the Golgi network-associated coated vesicles, in membrane tubules, and in the cisternae of the TGN. In addition viruses were seen in noncoated larger vesicles in the vicinity of dilated cisternae and dictyosomal stacks of the Golgi apparatus. In the Golgi area, AAV5 was still detectable even 22 h after infection. We conclude that the perinuclear signals seen by immunofluorescence microscopy (also described by other authors but controversial [5, 62]) are likely to represent AAV5 particles in the Golgi area, especially in the TGN and in TGN-associated vesicles. The immunofluorescence data also show that the electron microscopy data do indeed not reflect single cellular events since accumulation of AAV5 in cap-like structures was seen in almost all infected cells.

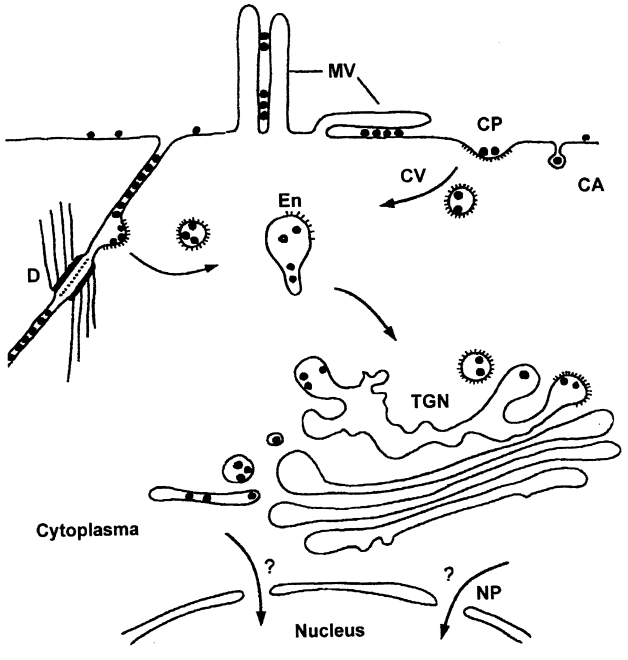

FIG. 7. Scheme of proposed endocytic pathway for AAV5 into HeLa cells. CA, noncoated pit; CP, coated pit; CV, coated vesicle; En, endosome; MV, microvilli; NP, nuclear pore; D, desmosome.

Targeting from the cell surface to the TGN sorting compartment via distinct and independent endosomal pathways has been reported for endocytosed proteins such as membrane proteins TGN38 and furin and protein toxins such as Shiga toxin and ricin (22, 31, 37, 38). TGN38 (22) and Shiga toxin (37) circumvent the late endocytic pathway and are transported from early endosomes directly to TGN. Furin passes through late endosomes on its way to the TGN (38), and studies with ricin showed the existence of several distinct routes from endosomes to the Golgi compartment (31).

The cellular mechanisms leading to parvovirus release from membranous compartments into the cytoplasm and translocation into the nucleus are still not understood. Since AAV5 particles are detectable within the TGN even at 22 h p.i., the final fate of AAV5 particles remains obscure. Being a central sorting compartment, the TGN is linked by anterograde and retrograde transport networks to cellular structures such as the endoplasmic reticulum, the plasma membrane, and late and early endosomes (for a recent review see reference 25). Recycling of AAV5 between the TGN and other compartments may be predicted from the detection of virus particles within Golgi-associated coated vesicles and within membrane tubules of roughly uniform size. These tubular structures (44) can be derived from either the Golgi complex or from endosomes and appear to function in transport (15).

Vesicular transport beyond the early endosome without prior release of virus particles into the cytoplasm and with capsid proteins being intact for several hours after virus uptake has been described for AAV2 and CPV (16, 27, 61) and is in agreement with our Western blot data for AAV5. Contrary to what is reported for AAV2 (16, 19), our protein degradation analysis does not point to significant loss of AAV5 capsid proteins for at least 6 h after infection and thus does not provide evidence of extensive degradation of incoming AAV5 by the proteasome system.

We did not identify intact virus particles in the cytoplasm but cannot exclude the possibility of their existence as such small particles might be obscured by the proteinaceous cytosolic meshwork. Since the antibody used in immunofluorescence detects capsids rather than individual capsid proteins, the faint fluorescence signals which we observed surrounding the nuclei might either represent still-membrane-bound AAV5 particles or particles that are not grossly modified before being transported to the nuclear membrane. However, as we never detected intact free AAV5 particles in the vicinity of the nuclear membrane or at nuclear pores in electron microscopy, some uncoating and loss of structural integrity cannot be excluded. The absence of any AAV5-specific immunofluorescence staining within the cell nucleus in our experiments suggests that AAV5 capsids may not enter in intact form. This is in contrast to the findings reported for AAV2 and for CPV, which claim detection of either small numbers (5, 62) or of about 90% of the particles (52) in the nucleus within a few hours after infection, thus suggesting that AAV2 and CPV enter the nucleus prior to uncoating.

It appears noteworthy that the observed pathway of entry may be the one used by the majority of virus particles but may not necessarily be the infectious pathway. Given the number of

virus particles required for detection and the high ratio of noninfectious to infectious particles found in virus preparations from infected cells, it may well be that the few infectious particles that are required for productive infection and thus the particular pathway they use are not detectable. Notwithstanding, demonstration of internalized viruses within the Golgi compartment points to the existence of cellular trafficking routes which have hitherto not been described as being involved in endocytic processes, either for AAV5 specifically or for viruses in general.

ACKNOWLEDGMENTS

We thank H. Spring for performing confocal microscopy and A. Wohlfahrt for correcting the manuscript.

REFERENCES

1. **Balague, C., M. Kalla, and W. W. Zhang.** 1997. Adeno-associated virus Rep78 protein and terminal repeats enhance integration of DNA sequences into the cellular genome. J. Virol. **71:**3299–3306.
2. **Bantel-Schaal, U., H. Delius, R. Schmidt, and H. zur Hausen.** 1999. Human adeno-associated virus type 5 is only distantly related to other known primate helper-dependent parvoviruses. J. Virol. **73:**939–947.
3. **Bantel-Schaal, U., and H. zur Hausen.** 1984. Characterization of the DNA of a defective parvovirus isolated from a genital site. Virology **134:**52–63.
4. **Bantel-Schaal, U., and H. zur Hausen.** 1988. Adeno-associated viruses inhibit SV40 DNA amplification and replication of herpes simplex virus in SV40-transformed hamster cells. Virology **164:**64–74.
5. **Bartlett, J. S., R. Wilcher, and R. J. Samulski.** 2000. Infectious entry pathway of adeno-associated virus and adeno-associated virus vectors. J. Virol. **74:**2777–2785.
6. **Basak, S., and H. Turner.** 1992. Infectious entry pathway for canine parvovirus. Virology **186:**368–376.
7. **Beck, S. E., L. A. Jones, K. Chesnut, S. M. Walsh, T. C. Reynolds, B. Carter, F. B. Askin, T. R. Flotte, and W. B. Guggino.** 1999. Repeated delivery of adeno-associated virus vectors to the rabbit airway. J. Virol. **73:**9446–9455.
8. **Berns, K. I.** 1996. *Parvoviridae*: the viruses and their replication, p 2173–2197. *In* B. N. Fields, D. M. Knipe, and P. M. Howley (ed.), Fields virology, 3rd ed. Lippincott-Raven Publishers, Philadelphia, Pa.
9. **Chao, H., Y. Liu, J. Rabinowitz, R. J. Samulski, and C. E. Walsh.** 2000. Several log increase in therapeutic transgene delivery by distinct adeno-associated viral serotype vectors. Mol. Ther. **2:**619–623.
10. **Chardonnet, Y., and S. Dales.** 1970. Early events in the interaction of adenoviruses with HeLa cells. I. Penetration of type 5 and intracellular release of the DNA genome. Virology **40:**462–477.
11. **Chiorini, J. A., F. Kim, L. Yang, and R. Kotin.** 1999. Cloning and characterization of adeno-associated virus type 5. J. Virol. **73:**1309–1319.
12. **Chiorini, J. A., L. Yang, Y. Liu, B. Safer, and R. M. Kotin.** 1997. Cloning of adeno-associated virus type 4 (AAV4) and generation of recombinant AAV4 particles. J. Virol. **71:**6823–6833.
13. **Chirmule, N., W. Xiao, A. Truneh, M. A. Schnell, J. V. Hughes, P. Zoltick, and J. M. Wilson.** 2000. Humoral immunity to adeno-associated virus type 2 vectors following administration to murine and nonhuman primate muscle. J. Virol. **74:**2420–2425.
14. **Davidson, B. L., C. S. Stein, J. A. Heth, I. Martins, R. M. Kotin, T. A. Derksen, J. Zabner, A. Ghodsi, and J. A. Chiorini.** 2000. From the cover: recombinant adeno-associated virus type 2, 4, and 5 vectors: transduction of variant cell types and regions in the mammalian central nervous system. Proc. Natl. Acad. Sci. USA **97:**3428–3432.
15. **De Figueiredo, P., D. Drecktrah, J. A. Katzenellenbogen, M. Strang, and W. J. Brown.** 1998. Evidence that phospholipase A_2 activity is required for Golgi complex and trans Golgi network membrane tubulation. Proc. Natl. Acad. Sci. USA **95:**8642–8647.
16. **Douar, A.-M., K. Poulard, D. Stockholm, and O. Danos.** 2001. Intracellular trafficking of adeno-associated virus vectors: routing to the late endosomal compartment and proteasome degradation. J. Virol. **75:**1824–1833.
17. **Duan, D., Q. Li, A. W. Kao, Y. Yue, J. E. Pessin, and J. F. Engelhardt.** 1999. Dynamin is required for recombinant adeno-associated virus type 2 infection. J. Virol. **73:**10371–10376.
18. **Duan, D., P. Sharma, J. Yang, Y. Yue, L. Dudus, Y. Zhang, K. E. Fisher, and J. F. Engelhardt.** 1998. Circular intermediates of recombinant adeno-associated virus have defined structural characteristics responsible for long-term episomal persistence in muscle tissue. J. Virol. **72:**8568–8577.
19. **Duan, D., Y. Yue, Z. Yan, J. Yang, and J. F. Engelhardt.** 2000. Endosomal processing limits gene transfer to polarized airway epithelia by adeno-associated virus. J. Clin. Investig. **105:**1573–1587.
20. **Erles, K., P. Sebokova, and J. R. Schlehofer.** 1999. Update on the prevalence of serum antibodies (IgG and IgM) to adeno-associated virus (AAV). J. Med. Virol. **59:**406–411.
21. **Georg-Fries, B., S. Biederlack, J. Wolf, and H. zur Hausen.** 1984. Analysis of proteins, helper dependence, and seroepidemiology of a new human parvovirus. Virology **134:**64–71.
22. **Ghosh, R. N., W. G. Mallet, T. T. Soe, E. McGraw, and F. R. Maxfield.** 1998. An endocytosed TGN38 chimeric protein is delivered to the TGN after trafficking through the endocytic recycling compartment in CHO cells. J. Cell Biol. **142:**923–936.
23. **Grimm, D.** 2000. Adeno-associated virus (AAV) serotypes as vectors for human gene therapy. Res. Adv. Virol. **1:**91–114.
24. **Grimm, D., and J. A. Kleinschmidt.** 1999. Progress in adeno-associated virus type 2 vector production: promises and prospects for clinical use. Hum. Gene Ther. **10:**2445–2450.
25. **Gu, F., C. M. Crump, and G. Thomas.** 2001. Trans-Golgi network sorting. Cell. Mol. Life Sci. **58:**1067–1084.
26. **Halbert, C. L., E. A. Rutledge, J. M. Allen, D. W. Russell, and A. D. Miller.** 2000. Repeat transduction in the mouse lung by using adeno-associated virus vectors with different serotypes. J. Virol. **74:**1524–1532.
27. **Hansen, J., K. Qing, and A. Srivastava.** 2001. Adeno-associated virus type 2-mediated gene transfer: altered endocytic processing enhances transduction efficiency in murine fibroblasts. J. Virol. **75:**4080–4090.
28. **Helenius, A., and N. Acheson.** Virus entry. *In* N. Acheson (ed.), Fundamentals of molecular biology. John Wiley & Sons, New York, N.Y., in press.
29. **Helenius, A., J. Kartenbeck, K. Simons, and E. Fries.** 1980. On the entry of Semliki Forest virus into BKH-21 cells. J. Cell Biol. **84:**404–420.
30. **Henley, J. R., H. Cao, and M. A. McNiven.** 1999. Participation of dynamin in the biogenesis of cytoplasmic vesicles. FASEB J. **13**(Suppl. 2)**:**243–247.
31. **Iversen, T.-G., G. Skretting, A. Llorente, P. Nicoziani, B. van Deurs, and K. Sandvig.** 2001. Endosome to Golgi transport of ricin is independent of clathrin and of the Rab9- and Rab11-GTPases. Mol. Biol. Cell **12:**2099–2107.
32. **Kartenbeck, J., H. Stukenbrok, and A. Helenius.** 1989. Endocytosis of simian virus 40 into the endoplasmic reticulum. J. Cell Biol. **109:**2721–2729.
33. **Keitel, V., J. Kartenbeck, A. T. Nies, H. Spring, M. Brom, and D. Keppler.** 2000. Impaired protein maturation of the conjugate export pump MRP2 as a consequence of a deletion mutation in Dubin-Johnson syndrome. Hepatology **32:**1317–1328.
34. **Kotin, R. M., M. Siniscalco, R. J. Samulski, X. D. Zhu, L. A. Hunter, C. A. Laughlin, S. K. McLaughlin, N. Muzyczka, M. Rocchi, and K. I. Berns.** 1990. Site-specific integration by adeno-associated virus. Proc. Natl. Acad. Sci. USA **87:**2211–2215.
35. **Laemmli, U. K.** 1970. Cleavage of structural proteins during the assembly of the head of bacteriophage T4. Nature **227:**680–685.
36. **Linden, R. M., and K. I. Berns.** 2000. Molecular biology of adeno-associated viruses. Contrib. Microbiol. **4:**68–84.
37. **Mallard, F., C. Antony, D. Tenza, J. Salamero, B. Goud, and L. Johannes.** 1998. Direct pathway from early/recycling endosomes to the Golgi apparatus revealed through the study of Shiga toxin B-fragment transport. J. Cell Biol. **143:**973–990.
38. **Mallet, W. G., and F. R. Maxfield.** 1999. Chimeric forms of furin and TGN38 are transported from the plasma membrane to the trans-Golgi network via distinct endosomal pathways. J. Cell Biol. **146:**345–359.
39. **Manning, W. C., S. Zhou, M. P. Bland, J. A. Escobedo, and V. Dwarki.** 1998. Transient immunosuppression allows transgene expression following readministration of adeno-associated viral vectors. Hum. Gene Ther. **1:**477–485.
40. **Mayor, H. D., S. Drake, J. Stahmann, and D. M. Mumford.** 1976. Antibodies to adeno-associated satellite virus and herpes simplex in sera from cancer patients and normal adults. Am. J. Obstet. Gynecol. **126:**100–104.
41. **McNiven, M. A., H. Cao, K. R. Pitts, and Y. Yoon.** 2000. The dynamin family of mechanoenzymes: pinching in new places. Trends Biochem. Sci. **25:**115–120.
42. **Monahan, P. E., and R. J. Samulski.** 2000. AAV vectors: is clinical success on the horizon? Gene Ther. **7:**24–30.
43. **Muramatsu, S., H. Mizukami, N. S. Young, and K. E. Brown.** 1996. Nucleotide sequencing and generation of an infectious clone of adeno-associated virus 3. Virology **221:**208–217.
44. **Novikoff, P. M., A. B. Novikoff, N. Quintana, and J. J. Hauw.** 1971. Golgi apparatus, GERL, and lysosomes of neurons in rat dorsal root ganglia, studied by thick section and thin section cytochemistry. J. Cell Biol. **50:**859–886.
45. **Parker, J. S. L., and C. R. Parrish.** 2000. Cellular uptake and infection by canine parvovirus involves rapid dynamin-regulated clathrin-mediated endocytosis, followed by slower intracellular trafficking. J. Virol. **74:**1919–1930.
46. **Ponnazhagan, S., X. S. Wang, M. J. Woody, F. Luo, L. Y. Kang, M. Nallari, N. C. Munshi, S. Z. Zhou, and A. Srivastava.** 1996. Differential expression in human cells from the p6 promoter of human parvovirus B19 following plasmid transfection and recombinant adeno-associated virus 2 (AAV) infection: human megakaryocytic leukaemia cells are non-permissive for AAV infection. J. Gen. Virol. **77:**1111–1122.
47. **Qing, K., C. Mah, J. Hansen, S. Zhou, V. Dwarki, and A. Srivastava.** 1999. Human fibroblast growth factor receptor 1 is a co-receptor for infection by adeno-associated virus 2. Nat. Med. **5:**71–77.

48. **Qiu, J., and K. E. Brown.** 1999. Integrin αVβ5 is not involved in adeno-associated virus type 2 (AAV2) infection. Virology **264:**436–440.
49. **Qiu, J., A. Handa, M. Kirby, and K. E. Brown.** 2000. The interaction of heparin sulfate and adeno-associated virus 2. Virology **269:**137–147.
50. **Rutledge, E. A., C. L. Halbert, and D. W. Russel.** 1998. Infectious clones and vectors derived from adeno-associated virus (AAV) serotypes other than AAV type 2. J. Virol. **72:**309–319.
51. **Samulski, R. J., X. Zhu, X. Xiao, J. D. Brook, D. E. Housman, N. Epstein, and L. A. Hunter.** 1991. Targeted integration of adeno-associated virus (AAV) into human chromosome 19. EMBO J. **10:**3941–3950. (Erratum, **11:**1128, 1992.)
52. **Sanlioglu, S., P. K. Benson, J. Yang, E. M. Atkinson, T. Reynolds, and J. F. Engelhardt.** 2000. Endocytosis and nuclear trafficking of adeno-associated virus type 2 are controlled by Rac1 and phosphatidylinositol-3 kinase activation. J. Virol. **74:**9184–9196.
53. **Siegl, G., R. C. Bates, K. I. Berns, B. J. Carter, D. C. Kelly, E. Kurstak, and P. Tattersall.** 1985. Characteristics and taxonomy of Parvoviridae. Intervirology **23:**61–73.
54. **Srivastava, A.** 1998. Delivery systems for gene therapy: adeno-associate virus 2, p. 257–288. *In* P. J. Quesenberry, G. S. Stein, B. G. Forget, and S. M. Weissman (ed.), Stem cell biology and gene therapy. Wiley-Liss, Inc. New York, N.Y.
55. **Stang, E., J. Kartenbeck, and R. G. Parton.** 1997. Major histocompatibility complex class I molecules mediate association of SV40 with caveolae. Mol. Biol. Cell **8:**47–57.
56. **Summerford, C., J. S. Bartlett, and R. J. Samulski.** 1999. $\alpha_V\beta_5$ integrin: a co-receptor for adeno-associated virus type 2 infection. Nat. Med. **5:**78–82.
57. **Summerford, C., and R. J. Samulski.** 1998. Membrane-associated heparan sulfate proteoglycan is a receptor for adeno-associated virus type 2 virions. J. Virol. **72:**1438–1445.
58. **Surosky, R. T., M. Urabe, S. G. Godwin, S. A. McQuiston, G. J. Kurtzman, K. Ozawa, and G. Natsoulis.** 1997. Adeno-associated virus Rep proteins target DNA sequences to a unique locus in the human genome. J. Virol. **71:**7951–7959.
59. **Velasco, A., L. Hendricks, K. W. Moremen, D. R. Tulsiani, O. Touster, and M. G. Farquhar.** 1993. Cell type-dependent variations in the subcellular distribution of alpha-mannosidase I and II. J. Cell Biol. **122:**39–51.
60. **Vicent-Lacaze, N., R. O. Snyder, R. Gluzman, D. Bohl, C. Lagarde, and O. Danos.** 1999. Structure of adeno-associated virus vector DNA following transduction of the skeletal muscle. J. Virol. **73:**1949–1955.
61. **Vihinen-Ranta, M., A. Kalela, P. Makinen, L. Kakkola, V. Marjomaki, and M. Vuento.** 1998. Intracellular route of canine parvovirus entry. J. Virol. **72:**802–806.
62. **Vihinen-Ranta, M., W. Yuan, and C. R. Parrish.** 2000. Cytoplasmic trafficking of the canine parvovirus capsids and its role in infection and nuclear transport. J. Virol. **74:**4853–4859.
63. **Walters, R. W., S. M. P. Yi, S. Keshavjee, K. E. Brown, M. J. Welsh, J. A. Chiorini, and J. Zabner.** 2001. Binding of adeno-associated virus type 5 to 2,3-linked sialic acid is required for gene transfer. J. Biol. Chem. **276:**20610–20616.
64. **Wistuba, A., S. Weger, A. Kern, and J. A. Kleinschmidt.** 1995. Intermediates of adeno-associated virus type 2 assembly: identification of soluble complexes containing Rep and Cap proteins. J. Virol. **69:**5311–5319.
65. **Xiao, W., N. Chirmule, S. C. Berta, B. McCullough, G. Gao, and J. M. Wilson.** 1999. Gene therapy vectors based on adeno-associated virus type 1. J. Virol. **73:**3994–4003.
66. **Yang, Q., M. Mamounas, G. Yu, S. Kennedy, B. Leaker, J. Merson, F. Wong-Staal, M. Yu, and J. R. Barber.** 1998. Development of novel cell surface CD34-targeted recombinant adeno-associated virus vectors for gene therapy. Hum. Gene Ther. **9:**1929–1937.
67. **Zabner, J., M. Seiler, R. Walters, R. M. Kotin, W. Fulgeras, B. L. Davidson, and J. A. Chiorini.** 2000. Adeno-associated virus type 5 (AAV5) but not AAV2 binds to the apical surfaces of airway epithelia and facilitates gene transfer. J. Virol. **74:**3852–3858.